Rock Mech. Rock Engng. (2000) 33 (1), 31–51

Rock Mechanics and Rock Engineering
© Springer-Verlag 2000
Printed in Austria

Dynamic and Static Stability Assessment of Rock Slopes Against Wedge Failures

By

H. Kumsar[1], **Ö. Aydan**[2], and **R. Ulusay**[3]

[1] Pamukkale University, Department of Geological Engineering, Kinikli Campus, Denizli, Turkey
[2] Tokai University, Department of Marine Civil Engineering, Orido, Shimizu, Japan
[3] Hacettepe University, Department of Geological Engineering, Ankara, Turkey

Summary

The stability of slopes during and after excavation is always of great concern in the field of rock engineering. One of the structurally controlled modes of failure in jointed rock slopes is wedge failure. The limiting equilibrium methods for slopes under various conditions against wedge failure have been previously proposed by several investigators. However, these methods do not involve dynamic assessments and have not yet been validated by experimental results. In this paper, the tests performed on model wedges under static and dynamic loading conditions are described and the existing limiting equilibrium methods are extended to take into account dynamic effects. The applicability and validity of the presented method are checked through model tests carried out under well controlled conditions and by actual cases studied by the authors, both in Turkey and Japan.

1. Introduction

One of the fundamental problems of engineering geology and geotechnical engineering is assessing and maintaining the stability of natural and man-made slopes. Usually natural slopes are stable when they are not disturbed by any external force, such as seismic and hydrostatic forces, blasting and surcharge loading. When slopes are excavated for highways, power plants, construction of buildings and open pit mining, they may become unstable. In these situations, stability assessments become crucial for the stability of engineering work and for economy. In competent rocks, the stability of many slopes is controlled by wedges (Fig. 1a and 1b) or slabs of intact rock bounded by weak discontinuities, usually joints, faults or shear zones. Attitude of discontinuities in relation to the slope face orientation determines the kinematic feasibility. The geometrical intersection of the discontinuity sets with each other and the orientation of the slope face leads to different types of structurally controlled slope instability.

Wedge failures are analysed using kinematical approaches and also limiting

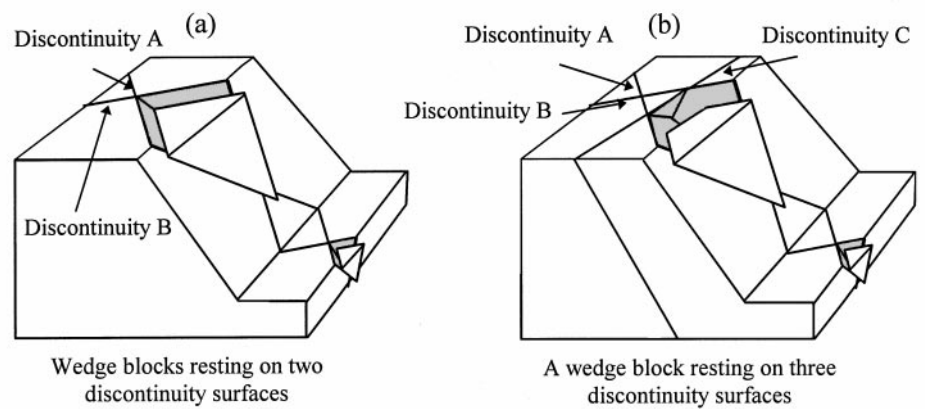

Fig. 1. Types of wedge failure

equilibrium methods. The limiting equilibrium method for wedge failure was first presented by Wittke (1967) and elaborated for different conditions by Kovári and Fritz (1975), and Hoek and Bray (1981). Although these methods consider water pressure, dynamic assessments are not included into the factor of safety computations. It is also noted that these previous approaches have not yet been validated by experimental results. The authors considered that re-assessment of the existing limiting equilibrium methods by means of model tests and numerical methods gives a confidence to geotechnical engineers during the design of slopes. In this paper, the authors describe the tests performed on the model wedges under static and dynamic loading conditions, and extend the limiting equilibrium method proposed by Kovári and Fritz (1975). Static tests involve dry and submerged conditions. The experimental results are used to check the validity of the presented limiting equilibrium method. In addition, the applicability of the presented method was also checked on the actual cases studied by the authors both in Turkey and in Japan. One of the cases was selected from an earthquake prone-region in Turkey to investigate the effects of the dynamic forces on the stability of the slope by back analysis.

2. Preparation of the Wedge Models

Concrete blocks were used as model materials in this study. Six types of wedge model moulds were set up and ordered to be prepared in a plastic factory in order to obtain smooth surfaces on the wedge models. Since these wedge models were designed for testing, and required to be stable at static condition before the tests, the plunge of the intersection line of discontinuities was kept between 28° and 31°. The horizontal projection of each intersection line is perpendicular to the slope strike. In order to check the influence of the wedge angle, as defined in Fig. 8, on the stability of the slope, half wedge angles were chosen between 23° and 56°, and the plastic wedge block models of which dimensions are given in Table 1 were prepared.

Table 1. Geometric parameters of the prepared model wedges

Wedge no.	Intersection angle – $i_a(^0)$	Half wedge angle $\omega_a(^0)$
TB1	29	56
TB2	29	51
TB3	31	45
TB4	27	36
TB5	30	30
TB6	30	23

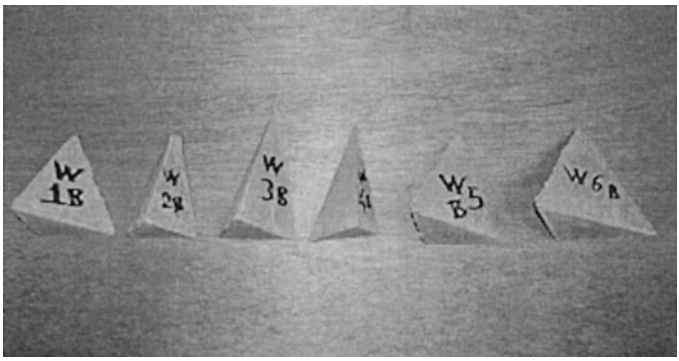

Fig. 2. Concrete wedge models used in the study

Base and wedge models were formed by using mortar, whose geomechanical parameters are similar to those of rocks. The composition of the mortar used for the preparation of the models includes 17.5 kN of fine sand, 3.5 kN of cement and 1.75 kN of water.

In order to model the wedge base and wedge blocks, wooden boxes with a length of 28 cm, a width of 14 cm and a depth of 12 cm were used. The preparation of the concrete models was carried out in two stages consisting of base and wedge model preparations. Base model preparation requires forming two discontinuity surfaces, that make a wedge failure surface, and the space for the wedge block volume. This was done by attaching specially prepared plastic wedge blocks having smooth surfaces and sharp edges at the sides of the boxes.

Plastic moulds were extracted from the base models after 8 hours, in order to minimize the damage to them during the extraction, so that discontinuity surfaces for wedges were obtained. By filling the rest of the space in each box with the mortar prepared earlier, the concrete wedge base blocks were modelled. After 24 hours, when the base and wedge models had become dry enough, the concrete wedge models were removed from the moulds. For each wedge type, three wedge models were prepared with the same geometry and material composition (Fig. 2). The base and wedge models then were cured for seven days to gain high strength.

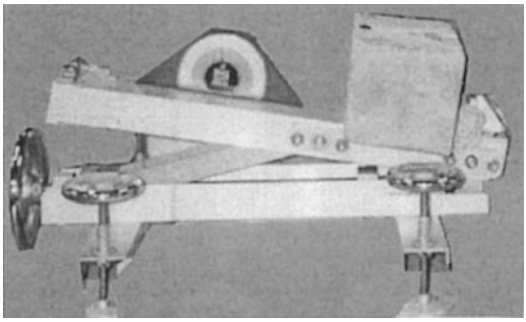

Fig. 3. Perspective view of the tilting test on a wedge model

3. Model Tests

A model testing program was undertaken to check the validity of the limiting equilibrium method to be presented in the next section. The concrete wedge models were tested under dynamic and static conditions. The static tests were carried out by considering dry and submerged conditions. The tests were briefly described in the following sections.

3.1 Static Tests

The friction angle between the concrete base block and the wedge models was determined from a tilting test, using a portable tilting device. Two concrete blocks, each having the same composition with the base and wedge models, were put on each other and the tilting angle at which the upper block slides on the lower block is assumed as the friction angle ($\phi = 35^\circ$), mobilised along the discontinuities.

3.1.1 Dry Tests

A portable tilting test device (Aydan et al., 1995) was used for the stability tests on the model wedges. After fixing the base blocks on the tilting test device, the wedge block models were assembled (Fig. 3). Then the base platform was gradually tilted by keeping the tilting speed as slow as possible. The inclination angle of each wedge block during sliding was recorded by means of an inclinometer. Each wedge block was tested three times to obtain the average inclination angle recorded during the sliding. For each wedge type, three wedge models were tested. The total number of static-dry wedge tests was 54.

3.1.2 Submerged Tests

The stability assessment of the wedge blocks was also carried out under submerged condition. The wedge base and wedge blocks were put in a water tank, which was

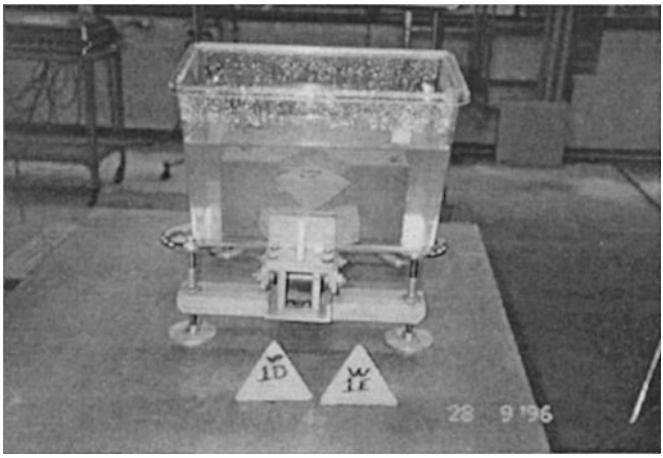

Fig. 4. Front view of the submerged stability test of a wedge model

filled with water up to a level at which all the model blocks were fully submerged (Fig. 4). The tilting test device was again used to measure the inclination angle of the base of the wedge models under submerged condition. Each wedge model was tested three times. For each wedge type, three concrete wedge models were tested and the average of the inclination angles at failure was assumed as a critical failure inclination angle for each wedge model.

3.2 Dynamic Tests

Rock slope failures may also occur under the influence of tectonic events in a region. Heavily jointed rock slopes may indicate that the region was subjected to active tectonic events in the past. If the tectonic events still continue from time to time, the slopes will be subjected to seismic forces. Even an engineering structure may not fail because of an earthquake shock; it may collapse as a result of a large scale wedge failure which is caused by the same earthquake shock. Dynamic forces can also result from blasting, traffic and machinery work near slopes. The influence of the seismic forces decreases the slope stability. Therefore, it is also an important task to investigate the dynamic stability of slopes.

Dynamic testing of the wedge models were performed in the laboratory by means of a one-dimensional shaking table, which moves along horizontal plane. The wave forms of the shaking table are sinusoidal, saw tooth, rectangular, trapezoidal and triangle. The shaking table has a square shape with 1m side length. The frequency of the wave to be applicable to the shaking table can range between 1 Hz and 50 Hz. The table has a maximum stroke of 100 mm, a maximum acceleration of 6 m/s^2 and a maximum load of 980.7 N.

Each wedge base block was fixed on the shaking table to receive same shaking with the shaking table during the dynamic test. The accelerations acting on the

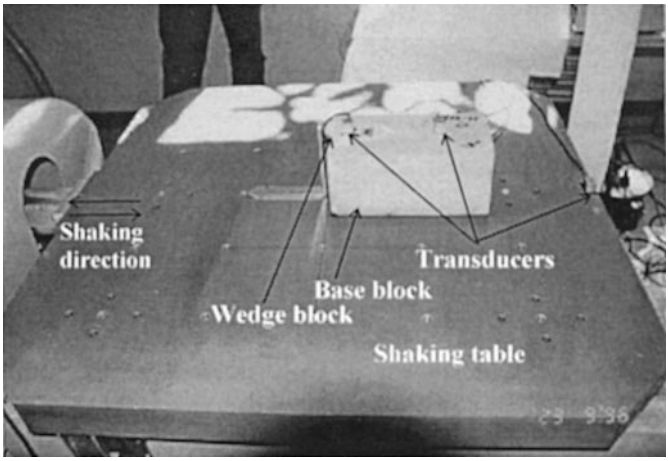

Fig. 5. A close up view from the shaking table during the experiment

shaking table, the base and wedge blocks were recorded during the experiment, and saved on a data file as digital data (Fig. 5). The reason for recording accelerations at three different locations during the experiments is to determine the acceleration at the moment of failure as well as any amplifications from the base to the top of the block. In fact, when the amplitude of input acceleration wave is increased, there must be a sudden decrease on the wedge block acceleration records during the wedge failure, while the others should be increasing.

The accelerographs may not completely record the acceleration data due to their insufficient sampling time of a record. Therefore, incomplete records may lead the investigator to misinterpret the acceleration at the time of failure. In Fig. 6 the acceleration records of shaking table, base and wedge blocks are shown for the dynamic stability test on the model numbered as TB1, as mentioned in Table 1. The wedge block failed just after 9^{th} second, as indicated in Fig. 6. The acceleration peaks of the shaking table and base blocks were incomplete at the moment of failure due to insufficient sampling time of the record. Finally, the failure moment is detected and the acceleration during failure is obtained by comparing the acceleration record graphs drawn for the shaking table, the base and the wedge blocks.

4. Limit Equilibrium Method

The approach proposed by Kovári and Fritz (1975) for the analysis of wedge failures is used and modified to take into account the possible loading conditions considered herein. The forces acting on a wedge block can be illustrated as shown in Fig. 7. If the force equilibrium in the directions of s, n and t is considered, the following equations are obtained.

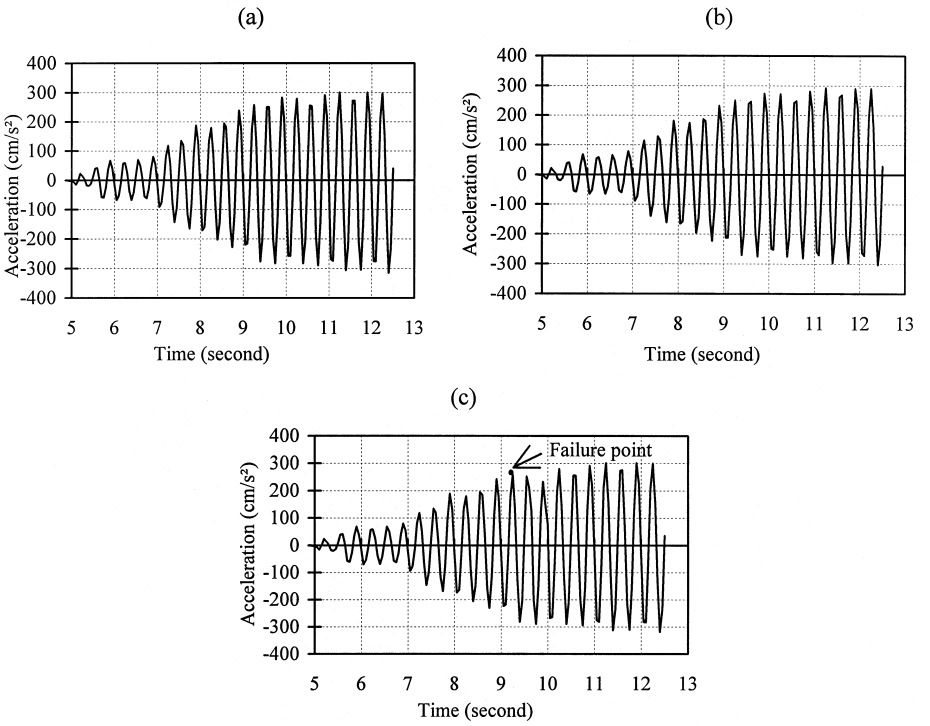

Fig. 6a–c. Example records of acceleration of the dynamic stability test on the wedge block numbered TB1C: **a** records on the shaking table; **b** records on the base block; **c** records on the wedge block

$$\sum F_s = W \sin i_a + E \cos(i_a + \beta) - U_s \cos i_a + U_t \sin i_a - S = 0, \tag{1}$$

$$\sum F_n = W \cos i_a - E \sin(i_a + \beta) + U_s \sin i_a + U_t \cos i_a - N = 0, \tag{2}$$

$$\sum F_t = -(N_1 + \alpha U_{b1}) \cos \omega_1 + (N_2 + \alpha U_{b2}) \cos \omega_2. \tag{3}$$

Where

$$N = (N_1 + \alpha U_{b1}) \sin \omega_1 + (N_2 + \alpha U_{b2}) \sin \omega_2 \tag{4}$$

and i_a is the plunge of the intersection line and α is Biot's coefficient. The weight of the wedge block can be written as

$$W = (1 - n) W_{br} + n W_{bw}, \tag{5}$$

where n is porosity, W_{br} is the weight of solid phase of the wedge block without regarding porosity, and W_{bw} is the weight of water contained in wedge block, S is shear force, N is the normal force acting perpendicular to the line of intersection in a plane, and E is the dynamic force, β and i_a are the inclinations of the dynamic force E and the line of intersection in turn. U_s and U_t are the water forces acting on the face and the upper part of the slope, respectively. ξ_1 and ξ_2 are the inclinations of the normal forces N_1 and N_2 acting normal to the surfaces A and B,

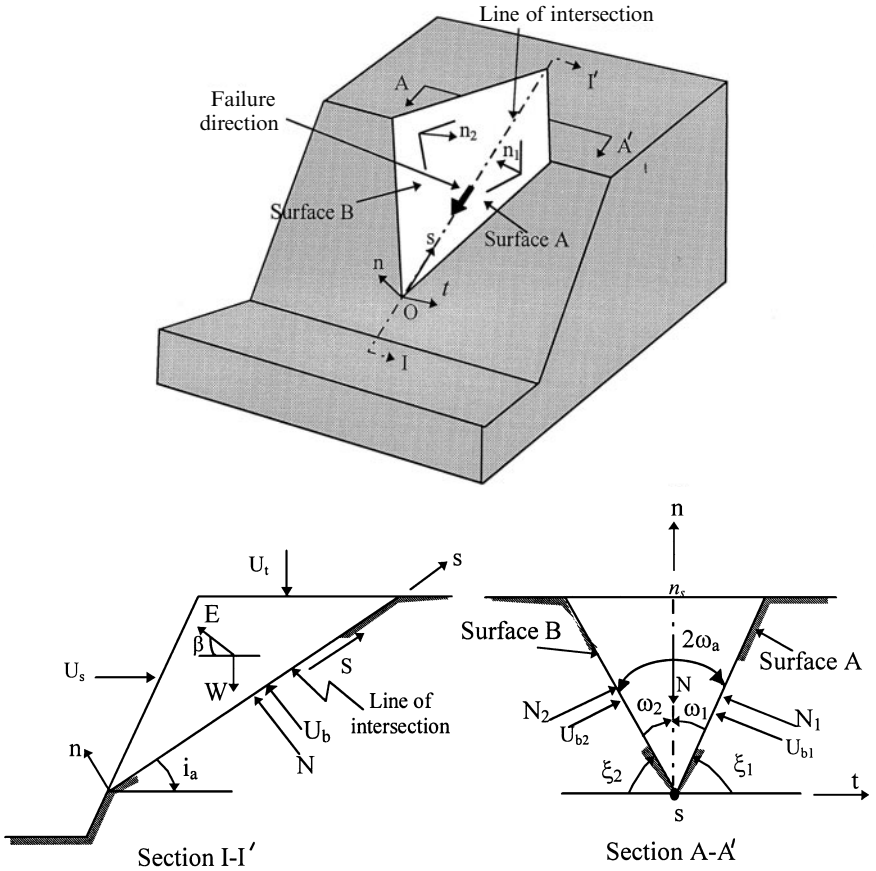

Fig. 7. Forces acting on a wedge block

respectively, ω_1 and ω_2 are the angles between the surface A and vertical and surface B and vertical in turn. The shear force components acting normal to the line of intersection on the surfaces of A and B are ignored in the Eqs. (2) and (3). This assumption is made by considering the fact that the movement on the normal direction to the line of intersection can be ignored. The only accelerations with the trend of the line of intersections are regarded. The sum of normal forces on plane 1 and plane 2 can be obtained from Eqs. (2) and (3) as

$$N_1 + N_2 = [W\cos i_a - E\sin(i_a + \beta) + U_s \sin i_a + U_t \cos i_a]\lambda - \alpha U_b, \tag{6}$$

where

$$U_b = U_{b1} + U_{b2} \tag{7}$$

and λ is called the wedge factor by Kovári and Fritz (1975) as

$$\lambda = \frac{\cos\omega_1 + \cos\omega_2}{\sin(\omega_1 + \omega_2)}. \tag{8}$$

Let assume that the failure planes obey Mohr-Coulomb yield criterion as given below:

$$T = (N_1 + N_2)\tan\phi + c(A_1 + A_2), \tag{9}$$

where c is cohesion, ϕ is friction angle, A_1 and A_2 are the area of plane 1 and plane 2, respectively.

The relationship between the dynamic force E, weight of the wedge block W, and the seismic coefficient η can be written as follow:

$$E = \eta W \tag{10}$$

and the factor of safety (SF) is given by the following expression,

$$\mathrm{SF} = \frac{T}{S} \tag{11}$$

Using Eqs. (1) to (4), the following expression for the factor of safety (SF) is obtained

$$\mathrm{SF} = \frac{[\lambda[W(\cos i_a - \eta\sin(i_a + \beta)) + U_s \sin i_a + U_t \cos i_a] - \alpha U_b]\tan\phi + c(A_1 + A_2)}{W(\sin i_a + \eta\cos(i_a + \beta)) - U_s \cos i_a + U_t \sin i_a}. \tag{12}$$

5. Special Conditions

Wedge slopes fail under the influence of various disturbing effects, such as seismic forces, surface loads, increasing pore pressure, water pressure in totally and partially submerged states, excavation at the toe in static dry case, etc. In the following sections, limiting equilibrium equations for wedge blocks in dry and submerged conditions without seismic loading, and dry case with seismic loading conditions are given.

5.1 Dry Condition with no Seismic Loading

Assuming that $\eta = 0$, U_s, U_t, U_{b1}, $U_{b2} = 0$, and $c = 0$, the following expression for the safety factor is obtained:

$$\mathrm{SF} = \lambda \frac{\cos i_a \tan\phi}{\sin i_a}. \tag{13}$$

Choosing SF = 1, the apparent friction angle ϕ^* due to the geometric configuration of the wedge is as follows:

$$\phi^* = \tan^{-1}(\lambda \tan\phi). \tag{14}$$

The maximum wedging effect is obtained when $\omega_1 = \omega_2 = \omega$.

5.2 Submerged Condition with no Seismic Loading

The effect of water has a vital importance on the behaviour of soils and rock masses on which engineering structures are built or excavated. Terzaghi (1925) introduced a concept of effective stress in order to express the mechanical effect of water on the behaviour of soils. This concept was also applied to rocks after that. Biot (1942), on the other hand, included the volumetric porosity n, and the ratio of the stiffness of the solid K_s and that of the bulk modulus K in his concept for general effective stress law.

Karaca et al. (1995) carried out a series of tests to clarify the applicability of the effective stress law for rock discontinuities. These experiments showed that Terzaghi-type effective stress law is generally applicable to throughgoing discontinuities. The factor of safety of a wedge block subjected to water forces in a submerged case can be written as:

$$\mathrm{SF} = \lambda.\frac{[W\cos i_a + U_s \sin i_a + U_t \cos i_a - \alpha(U_{b1}\sin\omega_1 + U_{b2}\sin\omega_2)]\tan\phi}{W\sin i_a - U_s\cos i_a + U_t \sin i_a}. \quad (15)$$

If α is chosen as 1, which corresponds to Terzaghi-type effective stress law, $c = 0$, the resulting equation by taking into account the geometry of the block will be obtained as

$$\phi^* = \tan^{-1}(\lambda \tan\phi). \quad (16)$$

This implies that the apparent friction angle of the block should be the same as both under dry and submerged conditions unless there is a chemical reaction between rock and water along sliding planes.

5.3 Dry Condition With Seismic Loading

Assuming that U_s, U_t, U_{b1}, $U_{b2} = 0$, and $c = 0$, the equation of the safety factor given below is obtained:

$$\mathrm{SF} = \lambda\frac{(\cos i_a - \eta\sin(i_a+\beta))\tan\phi}{\sin i_a + \eta\cos(i_a+\beta)}. \quad (17)$$

Choosing $\mathrm{SF} = 1$, the seismic coefficient η, at which the block slides, is as follows:

$$\eta = \frac{\lambda\cos i_a\tan\phi - \sin i_a}{\cos(i_a+\beta) + \lambda\sin(i_a+\beta)\tan\phi}. \quad (18)$$

6. Comparison and Discussion of the Experimental and Theoretical Results

The test results for assessing the stability of the wedge models under dynamic loading, dry static and submerged static states were compared with the theoretical predictions by using the presented limiting equilibrium method. For each wedge geometry, nine experimental results are used.

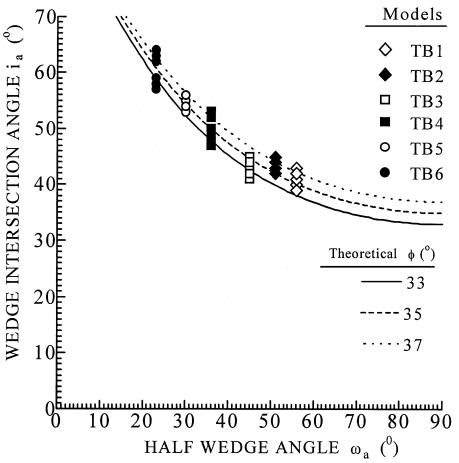

Fig. 8. Comparison of the dry-static model test results with theoretical solutions

In the case of dry static test, the plunge of the line of intersection during the failure of each wedge model is measured. This angle has two components: the plunge of the model (i_a) before tilting test, and the tilting angle of the model wedge surface at failure during tilting test, respectively. The sum of these two angles is called the plunge of the wedge model during the sliding in dry static test. Fig. 8 compares the theoretical predictions with the experimental results. From this comparison it can be stated that the limiting equilibrium method is generally valid when the strength of a discontinuity is purely frictional ($c = 0$).

The comparison of the submerged static test results of the wedge blocks and the theoretical estimation of the plunge during the failure of the wedge block for different values of the friction angle (ϕ) and zero cohesion (c), indicate that there is not a considerable difference among the failure intersection angles under static loading conditions (Fig. 9). This confirms that water pressure does not have an important influence on the stability of wedge models in submerged and $c = 0$ conditions, and Terzaghi-type effective stress law is applicable to rock discontinuities. However, if there is a chemical deterioration (such as softening of rock) on discontinuity surfaces due to the presence of water, the stability of a wedge block below water table may be influenced.

The results of the dynamic stability tests obtained from the wedge models were compared with the theoretical estimations (Fig. 10). The theoretical estimations were done by using Eq. (18) for the plunge of the line of intersection of each type of wedge model. The friction angle of the discontinuity surfaces, which was obtained from the tilting test, is taken 35°. The acceleration, that is required to make the wedge block unstable, is assessed for various half wedge angles. As seen from Fig. 10, the results of the dynamic stability tests on the wedge blocks are in a good agreement with those obtained from the presented limiting equilibrium method. The scattering in Fig. 10 may be attributed to the possible experimental errors in sample preparation and to the smoothness of the surfaces. It is suggested

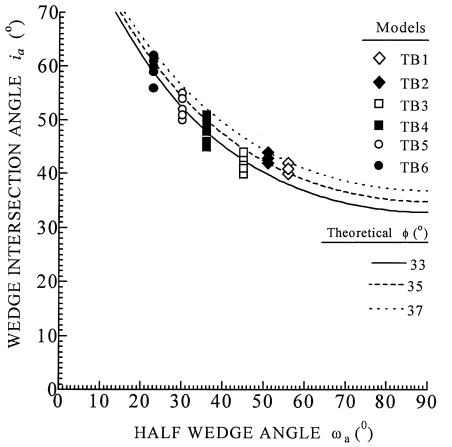

Fig. 9. Comparison of the submerged-static model test results with theoretical solutions

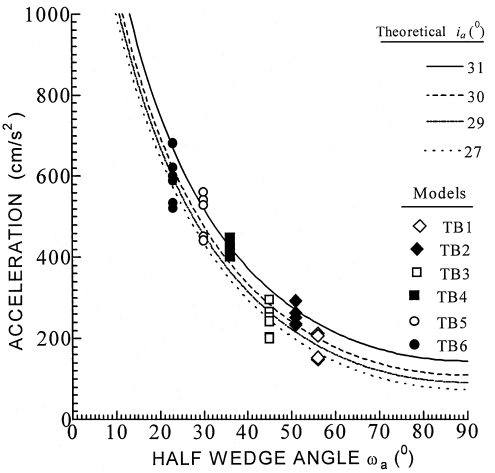

Fig. 10. Comparison of the dynamic model test results with theoretical solutions

that this method can be employed for the stability assessment of the slopes located in earthquake-prone regions.

7. Case Studies

A series of stability assessments of failed and stable wedge cases from Turkey and Japan were analysed by using the presented limiting equilibrium method. The cases from Turkey are, wedge failures in a very high bench at a strip coal mine, in an open museum in the Central Anatolia, in a quarry in Ankara Castle, and in an earthquake prone-region in western Turkey. A wedge failure in an active volcanic

mountain in Japan called Mayuyama was also assessed to check the validity of the presented method in this study.

7.1 Case 1: Wedge Failure at a Strip Coal Mine

One of the failures, which affected the operations at Eskihisar strip coal mine, SW Turkey, occurred in the form of a wedge failure. The wedge resulted from the intersection of a fault plane and a highly continuous joint (Fig. 11a). Tension cracks of large extent behind the crest after this failure suggested that the movement into the void was still continuing and a monitoring study was initiated. Then a second failure occurred.

On the basis of kinematical analysis of the slope (Fig. 11b) and the back analysis of the failure using the laboratory determined residual strength parameters of both discontinuities, it was concluded that the mode of failure of the previous major instability was wedge type, involving the fault and joint set numbered 4 (Ulusay, 1991). In this study, the geometrical parameters from the stereonet projection, and the weight of this wedge were calculated (Fig. 11a). The shear strength parameters of the fault plane were accepted to be mobilised and dropped to residual values during the failure (Fig. 11b). The back analysis yielded a safety factor of 0.93, which validates the limiting equilibrium method presented in this study. Monitoring station movement directions plotted (Fig. 11b) generally correspond to the trend of the line of intersection of the fault and the joint 1. This situation indicated that the wedge formed by $\hat{I}_f$, j_1 has been activated towards the void created by the previous failure.

7.2 Case 2: A Wedge Failure in an Open Museum

A wedge failure in a thick and soft tuff stratum was observed by the authors in Zelve Open Museum in Cappadocia Region in Central Anatolia. Two joints, intersecting each other, had slightly rough surfaces and formed a tetrahedral wedge (Fig. 12a).

Determination of the internal friction angle of these slightly rough joint surfaces was carried out by employing the criterion proposed by Barton and Choubey (1977). For this purpose, Schmidt Hammer rebound number and JRC value of the surfaces were determined, and the laboratory test results by Ulusay et al. (1997) carried out on these tuffs were also considered. Calculations yielded an internal friction angle of 30°. The kinematical analysis of the wedge with its geometrical parameters is given in Fig. 12b. The analysis of the failure using the presented method resulted in a factor of safety less than unity, which emphasises that the wedge block has already failed.

7.3 Case 3: Wedge Failure near Ankara Castle

A very old wedge failure in a jointed andesite rock mass near Ankara Castle in Bent Deresi region of Ankara City was investigated by the authors. Two discon-

(a)

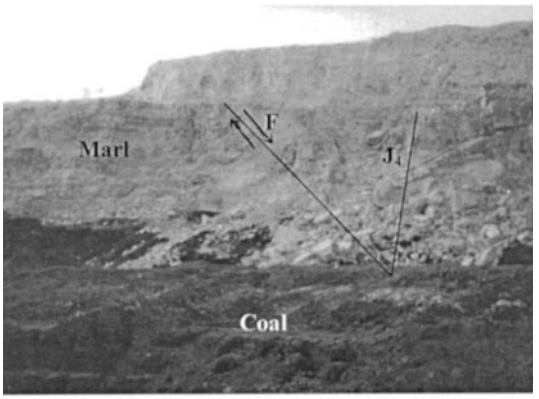

Parameter	Value
ω_1 (degree)	5.6
ω_2 (degree)	68
i_a (degree)	50
A1 (Joint surface area on wedge, m^2)	18.5
A2 (Fault surface area on wedge, m^2)	56.2
W (Weight of the wedge block, kN)	983

(b)

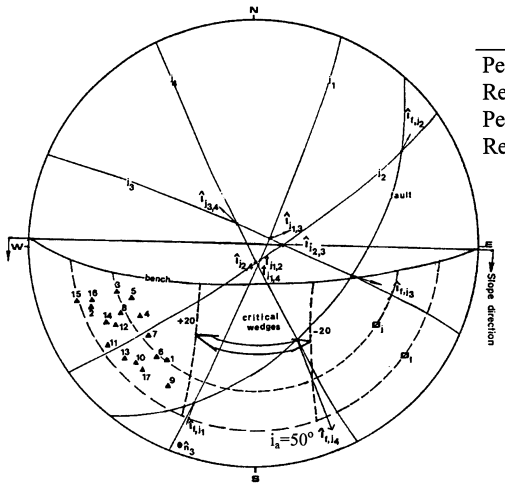

Parameter	Fault plane	Joint surface
Peak cohesion (kPa)	18.0	8.7
Residual cohesion (kPa)	5.5	3.6
Peak friction angle (°)	26.0	33.4
Residual friction angle (°)	17.6	31.8

3 Monitoring station movement direction

$i_{1,3}$ Structural intersections

$\hat{n}_3$: Pole plot

j : Joint
f : Fault
ϕ : Internal friction angle
i_a : Plunge of intersection line

Fig. 11a,b. Case 1: **a** general view of the wedge failure and the geometrical characteristics of the wedge; **b** kinematical analysis of possible lines of intersection and plots of monitoring data for Case 1 and shear strength parameters of the discontinuities involved by the wedge (after Ulusay, 1991)

tinuity surfaces dipping to each other formed a wedge surface within andesite (Figs. 13a and b). On the top of this wedge failure there is a house. The line of intersection, which was obtained from the kinematic analysis of the wedge failure shown in Fig. 13c, is greater than the friction angle and smaller than the slope angle.

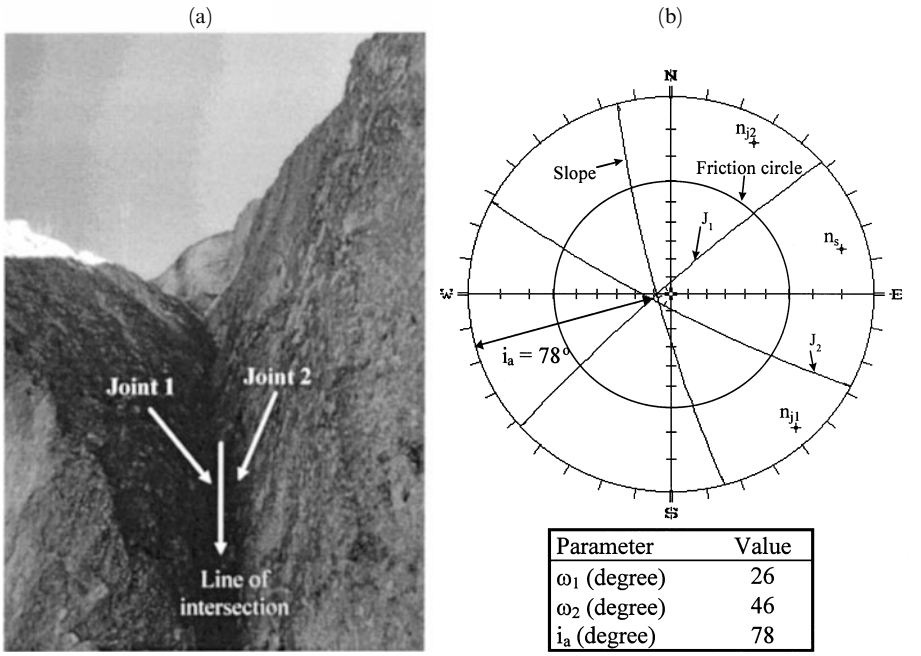

Parameter	Value
ω_1 (degree)	26
ω_2 (degree)	46
i_a (degree)	78

Fig. 12a,b. Case 2: **a** a wedge failure in Zelve at Cappadocia; **b** its kinematical analysis and geometrical characteristics

Under these conditions the wedge block is expected to be unstable. In the analysis, a friction angle of 30° determined from laboratory tests on joint samples by Ercanoglu (1997) was used. The stability assessment of the wedge block under dry-static condition was carried out by using the suggested method in this paper. The safety factor of the slope was found as 0.73, which clarifies that the slope has already failed.

7.4 Case 4: Wedge Failure at an Earthquake-prone Area

The town of Dinar is located at an earthquake-prone area in the western Turkey. An earthquake with a magnitude of 6.0 occurred in Dinar and its vicinity on October 1, 1995. During this disaster 90 people lost their lives and many houses collapsed and were damaged.

After the earthquake, field studies were carried out and a wedge failure was observed northeast of Kizilli Village near Dinar. This failure is located at the fault zone of Dinar (Fig. 14a). A kinematical analysis was done to determine the necessary wedge parameters for the stability assessment of the wedge block (Fig. 14b). The internal friction angle of the joint surfaces was determined by performing a simple tilting test in the field and found as 41°.

A back analysis of the wedge failure, using the proposed method, was carried out to check the influence of the seismic force due to Dinar earthquake on the

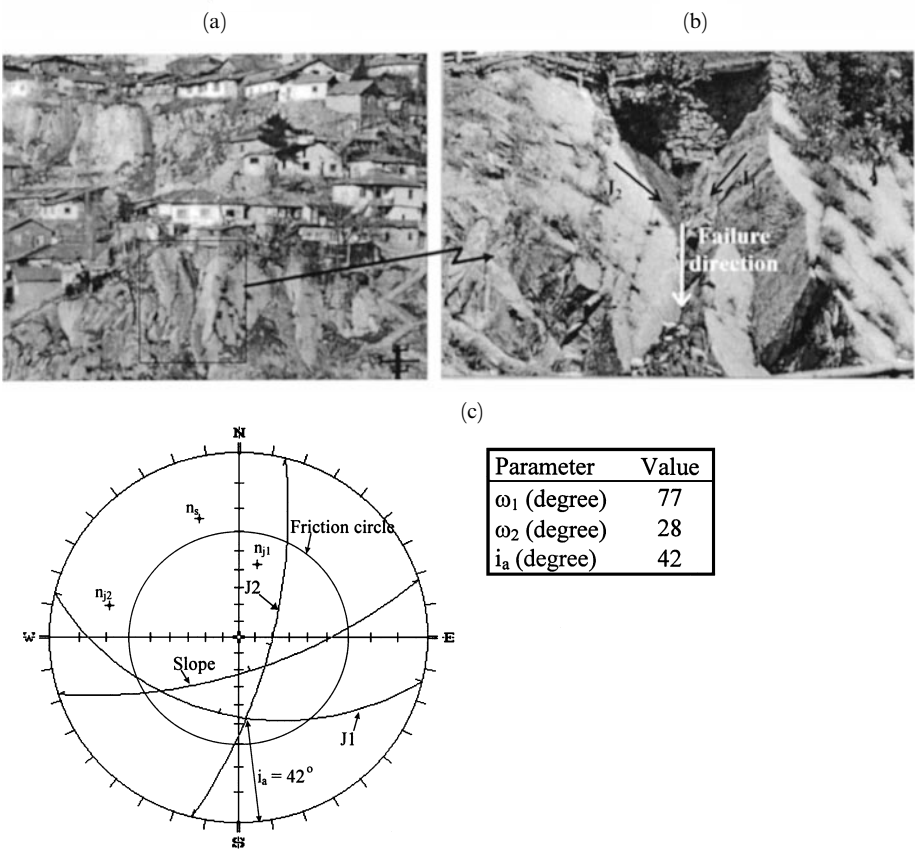

Parameter	Value
ω_1 (degree)	77
ω_2 (degree)	28
i_a (degree)	42

Fig. 13a–c. Case 3: **a** view of the wedge failure near Ankara Castle; **b** close up view from the wedge near Ankara Castle; **c** the kinematical analysis and the geometrical characteristics of the wedge

stability of the wedge block by considering static conditions. A factor of safety of 2.02 was obtained, which indicates that the wedge block is stable under static conditions. Therefore, a second analysis which takes dynamic conditions into account was performed by using the a_{max} value in EW direction (Aydan and Kumsar, 1997), given in Fig. 14. The value of the safety factor for this direction was 0.99. This result revealed that the slope instability was initiated when the earthquake occurred on October 1, 1995.

7.5 Case 5: Wedge Failure of Mt. Mayuyama in 1792

Mt. Mayuyama in Japan failed following an earthquake about 8 pm and resulted in the loss of 15000 people during a volcanic activity of Unzen volcanos in 1792. A slope failure also occurred during this disaster. The authors carried out a series of back analyses considering different conditions to discuss the mechanism and the model of this wedge type slope failure.

(a)

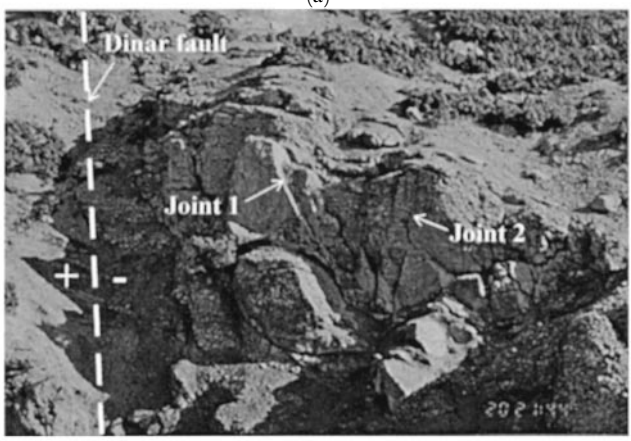

(b)

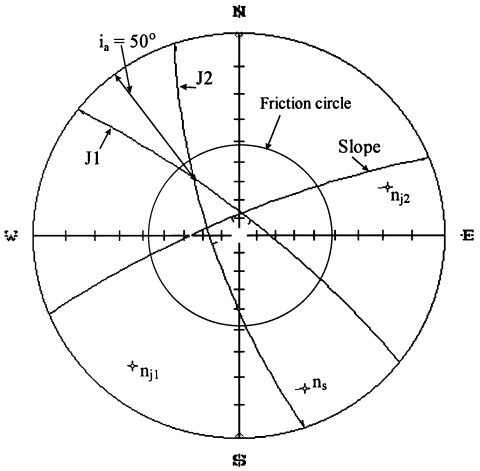

Parameter name	Value
ω_1 (degree)	17
ω_2 (degree)	25
i_a (degree)	50
Friction angle (degree)	40.8
β (degree)	0
a_{max} in NS direction (cm/s^2)	282
a_{max} in EW direction (cm/s^2)	324

Fig. 14a,b. Case 4: **a** the wedge failure occurred northeast of Kızıllı Village (Dinar) after the 1995 earthquake; **b** the kinematical analysis and the geometrical characteristics of the wedge

There are three different explanations of the failure of Mt. Mayuyama (Misawa et al., 1993):

1. Failure due to earthquake,
2. Failure due to gas pressure of heated ground water, and
3. Failure due to liquefaction of an underlying sandy layer.

Four cross-sections of the failed body are given in Fig. 15. From these sections it was concluded that there are three distinct failure planes, namely J_1, J_2 and J_3, and their projections on a lower hemisphere Schmidt net and wedge parameters for the stability assessment of the wedge block are given in Fig. 16.

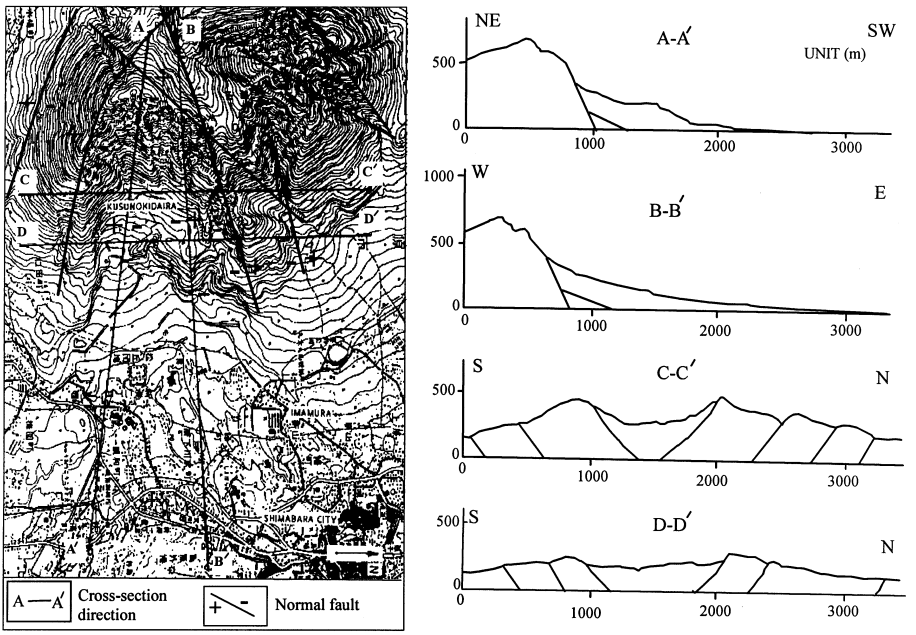

Fig. 15. Present topography and cross-sections of the close vicinity of Mt. Mayuyama (after Misawa et al., 1993)

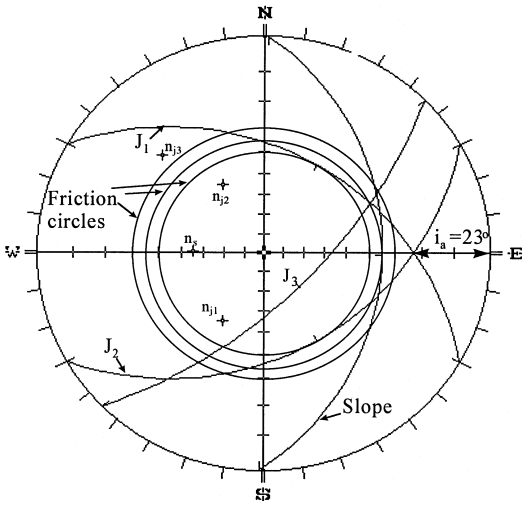

Parameter	Value
ω_1 (degree)	54
ω_2 (degree)	54
i_a (degree)	23

Fig. 16. Kinematical analyses of the wedge blocks at Mt. Mayuyama and the geometrical characteristics of the wedge

The planes J_1 and J_2 are the planes which should be developed long time (Ohta, 1987). However, the plane J_3 was considered to have developed during the volcanic activity and associated earthquake in 1792, since there is thin vegetation

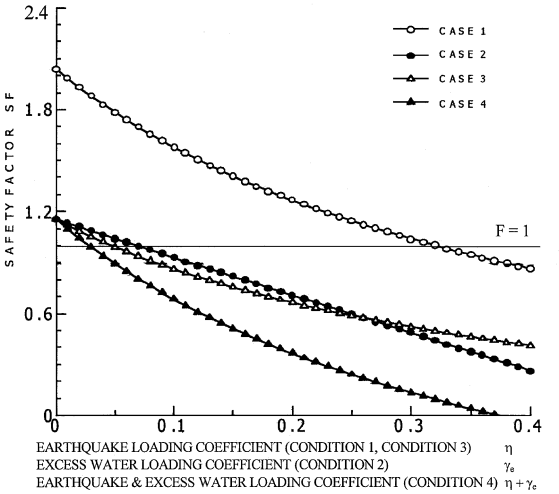

Fig. 17. Comparison of different case results for the wedge failure at Mt. Mayuyama

on this surface (Misawa et al., 1993). There are two possible wedge failures as shown in Fig. 16. Since the dip of the intersection of the planes J_1 and J_2 is greater than the slope angle, the wedge failure along these discontinuity planes is not kinematically possible. On the other hand the wedge failure on planes J_1 and J_3 is the most likely as the plunge of the intersection line daylights on the slope face. The geometrical parameters of the wedge were determined and given in Fig. 16.

A series of stability calculations were carried out by considering four different conditions (Fig. 17):

Condition 1: Rock mass is dry and earthquake force is only applied by increasing η from 0.0 to 0.5 with $c = 0$; $U_s = 0$; $U_t = 0$; $U_b = 0$; $\alpha = 1$; $\beta = 0$.

Condition 2: Rock mass is assumed to be subjected to only uplift fluid pressure acting on the discontinuity planes with $c = 0$; $U_s = 0$; $U_t = 0$; $\alpha = 1$; $\eta = 0$. The fluid pressure was assumed to consist of two parts: static fluid pressure ($U_{bs} = \gamma_s W$) and excess fluid pressure ($U_{be} = \gamma_e W$). The static fluid pressure coefficient (γ_s) is assumed to correspond to a fully saturated situation with a value of 0.4. The value of the excess fluid pressure coefficient (γ_e) was increased from 0.0 to 0.5.

Condition 3: Rock mass is assumed to be subjected to static fluid pressure and the earthquake force with $c = 0$; $U_s = 0$; $U_t = 0$; $\alpha = 1$. The fluid pressure was kept constant during the increase of the earthquake force.

Condition 4: Rock mass is assumed to be subjected to both the fluid pressure and earthquake force $c = 0$; $U_s = 0$; $U_t = 0$; $\alpha = 1$. The initial value of fluid pressure is equal to its static value. Then, excess fluid pressure and earthquake force increased by the same amount.

The results of the calculations for Condition 1 indicate that the seismic intensity (η) should be 0.36 to initiate the failure. Considering the magnitude of the earth-

quake at the time of failure, it is not possible that the mountain can fail without the effect of fluid pressure.

The mountain should be stable under the fully saturated condition according to the calculation results for Condition 2. However, if the excess pressure is to occur, the mountain failure could be initiated when the excess fluid pressure is 0.12 times the dead weight of the wedge body. If the excess fluid pressure is due to the heating of groundwater by the magma, the mountain failure is possible.

If the rock mass is fully saturated without generation of excess fluid pressure (Condition 3), the increase of seismic intensity η can also cause the failure of the mountain for a value of 0.08. If the Condition 4 is considered, the failure of the mountain can occur for a value of 0.05.

At the time of failure, an earthquake did happen and the hot water did spout from the ground. Therefore, it is most likely that the forces due to the earthquake and the fluid pressure caused by the gravity, shaking and heating of the groundwater could be the main reasons for the failure of the mountain. Nevertheless, it should be kept in mind that the observation of the hot water spewing out of the ground near the coast may also be caused by the energy dissipation released during the frictional sliding of the failing mountain.

8. Conclusions

The stability assessments of the wedge models were performed under dynamic and static loading conditions. While dynamic tests were carried out by using one dimensional shaking table under dry condition; the static tests were performed under two different conditions; namely dry and submerged. A portable tilting machine was used for the static tests. In submerged tests the base and wedge blocks were put in a water tank, which was filled with water. The experimental results were compared with the theoretical estimations. In static tests, the calculated results are in good agreement with the experimental results for static and dynamic states when the shearing forces between the discontinuity surface were controlled by friction only. There is not a great deal of influence of water pressure in submerged condition under static loading conditions. This proves that Terzaghi-type of effective stress law is applicable to rock discontinuities. The estimated accelerations for $F = 1$ condition by using the presented limit equilibrium method are also close to the accelerations obtained from the dynamic tests. Therefore, the presented method can also be applied for the dynamic stability assessment of wedge failures.

The stability assessment of the wedge cases was carried out under static-dry condition, and the stability conditions of the wedges were determined by using the presented limiting equilibrium method. A back analysis of a wedge failure at an earthquake-prone area showed that the wedge block was stable under static state. When a seismic force, resulting from an earthquake shock occurred in Dinar in Turkey in October 1995, was introduced, the slope lost its stability. Four different conditions were considered in a case study of a wedge failure in an active volcanic mountain. The main reasons for the instability of the wedge were estimated as the earthquake and the fluid pressure caused by the gravity, shaking and heating of

the groundwater. These case studies also show the validity of the limiting equilibrium approach.

References

Aydan, Ö., Kumsar, H. (1997): A site investigation of Dinar earthquake of October 1, 1995. Turkish Earthquake Foundation, TDV/DR 97-003, Istanbul, Turkey, 115 pp.

Aydan, Ö., Shimizu, Y., Kawamoto, T. (1995): A portable system for in-situ characterization of surface morphology and frictional properties of rock discontinuities. Proc., 4th Int. Symp. on Field Measurements in Geomechanics, Bergamo, Italy, 463–470.

Barton, N. R., Choubey, V. (1977): The shear strength of rock joints in theory and practice. Rock Mech. 10, 1–54.

Biot, A. M. (1942): The theory of three dimensional consolidation, J. Apply. Phys. 12, 155–165.

Ercanoglu, M. (1997): Altindag (Ankara) yerlesim bölgesindeki andezitlerde olasi sev duraysizlik modellerinin incelenmesi ve duraysizlik haritasinin olusturulmasi. Yüksek Lisans Tezi, Hacettepe Üniversitesi Fen Bilimleri Enstitüsü, Ankara, 83 pp (in Turkish).

Hoek, E., Bray, J. W. (1981): Rock slope engineering, 3rd edn. Institute of Mining and Metallurgy, London, 358 pp.

Karaca, M., Sezaki, M., Aydan, Ö. (1995): Assessing the mechanical response of rock structures subject to water forces. Proc., 35th US Rock Mechanics Symp., Lake Tahoe, 335–340.

Kovári, K., Fritz, P. (1975): Stability analysis of rock slopes for plane and wedge failure with the aid of a programmable pocket calculator. 16th US Rock Mech. Symp., Minneapolis, USA, 25–33.

Misawa, Y., Aydan, Ö., Hamada, M. (1993): A consideration on the failure of Mt. Mayuyama in 1792 from rock mechanics view point. Proc., Int. Symp. on Assessment and Prevention of Failure Phenomena in Rock Engineering, Istanbul, Turkey, 871–877.

Ohta, K. (1987): Geological structure of Unzen Volcano and its relation to the volcanic phenomena. Chidanken Symp. 33 (7) 71–85 (in Japanese).

Terzaghi, K. (1925): Erdbaumechanik auf bodenphysikalischer Grundlage. F. Deuticke's Verlag, Leipzig.

Ulusay, R. (1991): Geotechnical evaluations and deterministic design considerations for pitwall slopes at Eskihisar (Yatagan–Mugla) strip coal mine. PhD Thesis, Middle East Technical University, Ankara, Turkey, 340 pp.

Ulusay, R., Gökçeoglu, C., Binal, A. (1997): Physical and mechanical properties of the tuff samples from Cappadocia Region. Report of Hacettepe University, Geological Engineering Department, 32 pp.

Wittke, W. (1967): Influence of the shear strength of joints on the design of prestressed anchors to stabilize a rock slope. Geotechnical Conference, Oslo, Paper No. 4.11, 311–318.

Authors' address: Dr. Halil Kumsar, Pamukkale University, Department of Geological Engineering, Kinikli Kampusu, TR-20017 Denizli, Turkey.